

Resolving Challenges in Analyzing Iron-Rich Samples by X-Ray Diffraction

Salah Al-Ofi^{1*}, Shouxiang Ma²

¹Baker Hughes, Dhahran Technology Center 4.0, 31952 Dhahran, Saudi Arabia

²Saudi Aramco, Reservoir Description & Simulation Department, 31952 Dhahran, Saudi Arabia

Abstract. Rock mineralogy is the foundation of formation evaluation and X-ray diffraction (XRD) is considered the gold standard for rock mineralogical analysis. The main objective of this study is to address challenges in analyzing iron rich rocks using the commonly used XRD method, by systematically study sample preparations, measurement procedures, raw data processing, and data interpretation and quantification. An XRD test can be described in three steps: sample preparation and testing, mineral identification, and mineral quantification. Rock samples used in this study are from US subsurface Chelsea sandstone (CSST), consisting of shales, shaly sands, and sideritic sandstone. To prepare for a XRD test, core plugs were pulverized using the traditional pestle and mortar, planetary ball mill machine, and Mortar Grinder RM 200. The sample powders were analyzed with the commonly used Rigaku Ultima IV and PANalytical Empyrean diffractometer systems. X-ray tubes with copper Cu anode materials were utilized as the radiation source for the two systems. Jade Software was used to identify mineral phases using ICDD PDF4+ library. The mineral phase quantification was performed using Rietveld refinement method in Jade software and utilizing three different libraries: ICDD PDF4+, MDI, and AMCSD, and different data simulation models: Current Background, Refinable Polynomial and Variable Spline. Results show that high background noise affects measurement due to secondary copper radiation associated with the content of sideritic in the sample as they fluoresce and create polychromatic radiation. The more siderite (FeCO₃) presence in the sample the higher the background level which distorts other mineral phases present in the sample. The diffractogram from the shaly sandstone showed multiple mineral phases which are repressed in the mixed samples diffractogram of 50% of shaly and sideritic sandstone. Also, our investigation showed the influence of both mineral library and fitting model section on the accuracy of minerals quantification. Results show Cu radiation diffractograms can be a source of measurement uncertainty that need to be accounted for by careful selection of mineral library and fitting model. This observation is used to enhance the quality of XRD analysis of iron rich rocks using copper radiation.

1 Introduction

Laboratory X-ray diffraction (XRD) analysis is an important test for characterization of geologic formations. It is a common tool that provides a fast identification of minerals and mineral quantification. The information provided by an XRD test is critical for formation evaluation [1], which has a significant impact in oil and gas exploration and development [2-6]. Equally important is the knowledge of the mineral composition within precipitates from corrosion and scales that affect tools and well performance [7,8].

1.1 Theoretical Background

XRD is based on constructive interference of monochromatic X-rays and a crystalline sample of specially prepared powder material. These X-rays are generated by a cathode ray tube, filtered to produce monochromatic radiation, collimated to concentrate, and directed toward the sample. The interaction of the incident rays with the sample produces constructive interference (and a diffracted ray) when conditions satisfy Bragg's law in Eq. 1 below:

$$n\lambda = 2d \sin \theta \quad (1)$$

Where,

λ = incident X-ray wavelength

n = an integer (i.e. 1, 2, 3, etc.)

d = distance between lattice planes

θ = angle between the incident X-ray and the lattice plane

The Bragg's law relates the wavelength of electromagnetic radiation to the diffraction angle and the lattice spacing in a crystalline sample, Fig. 1. These diffracted X-rays are then detected, processed, and counted. By scanning the sample through a range of 2θ angles, all possible diffraction directions of the lattice should be attained due to the random orientation of the powdered material. Conversion of the diffraction peaks to d-spacings allows identification of the mineral because each mineral has a set of unique d-spacings. Typically, this is achieved by comparison of d-spacings with standard reference patterns [9,10].

In conducting an XRD test, there may be three common challenges, which are mostly analyst dependent, including sample preparation, identify the right minerals and quantify identified minerals. Additional challenges may be associated with the instrumentation available to perform the test.

* Corresponding author: salah.al-ofi@bakerhughes.com

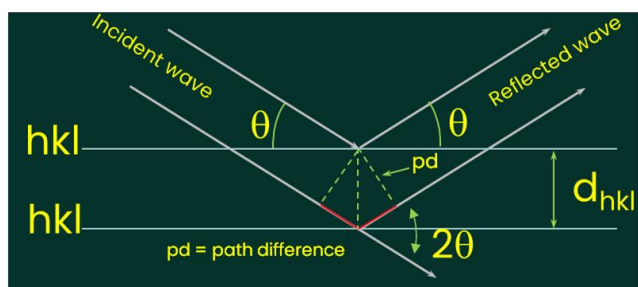


Fig. 1 Showing XRD bases, hkl is the lattice plane.

In this paper, we aim to present a detailed study into the possibility of reducing XRD data uncertainty by:

1. Investigating how sample preparation affects XRD analysis and establishing the best procedure.
2. Studying and establishing a consistent protocol in mineral identification.
3. Determining the best mineral quantification method.

2 Methodology

In this study, the outcrop Indiana Limestone (ILST), Fontainebleau sandstone (FBST) and Chelsea (CSST) sandstone samples from United States of America were used. Both ILST and FBST are clay-free rocks, while CSST is mixture of shale, shaly and sideritic sandstone. Also, a multiminerall mixed sample (MIX1) from middle east outcrop is included.

2.1 Sample Preparation and Data Acquisition

To study effect of sample preparation, we evaluated impact of grinding machine, grinding time, and data acquisition following the below steps.

1. Sampling: The outcrop samples were acquired as core plugs and XRD samples were selected from end trims of core plugs (Fig. 2).
2. Cleaning: Samples were cleaned using Soxhlet extraction using methanol, to remove any dusty precipitates.
3. Crushing: Mortar and pestle were used to break sample into pieces (Fig. 3). A tensile test machine was used for crushing tougher samples such as those of FBST rocks.
4. Grinding: The crushed sample was grinded for five minutes into powder, with a planetary ball mill machine and the Mortar Grinder RM 200.
5. Re-grinding: To reduce the lithological grainy effect and to ensure that average grain size at about 10 μm , about 2 g was collected for re-grinding.
6. Data acquisition: About 1.5 g of the re-grinded pulverized sample was loaded into Rigaku Ultima IV machine, and 1 g was loaded into the Epyrean, Panalytical machine for the XRD test, with the below conventional data acquisition parameters (Table 1). It is noted that iron-rich, if known, samples may require more dwell time to increase diffractogram quality.



Fig. 2 Illustration of rock sample end trims.



Fig. 3 Illustration of crushed sample using mortar and pestle.

Table 1 Instruments parameters and settings for data collection

Parameter	Rigaku	Panalytical
2 θ - Start (deg)	4.6	4
2 θ - End (deg)	60	70
Step Size (deg)	0.02	0.01
Data Point	2771	5027
Time/cycle (min)	60	20
No of Cycle	1	2
Total Time (min)	60	40
Sample Loading - Stages	10	45
Sample Loading - Technique	Front	Back

2.2 Mineral Phase Identification

The Jade Software was used to identify mineral phases using ICDD PDF4+ library, using line match points between measured data and ICDD PDF4+ database. Other libraries are investigated in the phase quantification section.

2.3 Mineral Phase Quantification

To quantify minerals weight percentage, we utilized three different libraries and quantification/simulation models in Jade software. A summary of commonly used phase quantification methods is shown in Fig. 4 [11, 12]. In this study, we considered the Rietveld refinement method. For the simulation models used in Jade software, there are three background fitting models to be studied: Current Background, Refinable Polynomial and Variable Spline.

Regarding the libraries used, three main sources were evaluated in this study:

- ICDD PDF4+: International Center for Diffraction Data.
- MDI: Material Data Incorporated.

- AMCSD: American Mineralogist Crystal Structure Database.

The essential simulation parameters are defined by Eq. 2:

$$I_{hkl} = k \times L_p \times T \times A \times G \times m \times F_{hkl}^2 \quad (2)$$

Where,

I_{hkl} = the integrated intensity of a reflection with Miller indices (hkl).

k = a scaling constant related to the intensity of X-ray beam.

L_p = the Lorentz & X-ray polarization factor which is dependent on the Diffraction Geometry.

T = the overall temperature factor of the structure.

A = the absorption correction for flat and thin specimen.

G = the preferred orientation correction.

m = the reflection multiplicity.

F_{hkl} = the structure factor derived from the packing (i.e. Fourier transform) of all atoms in the unit cell.

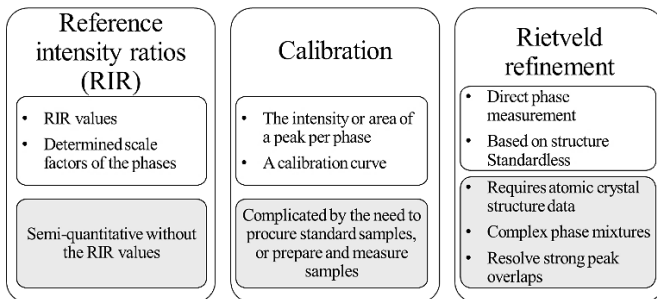


Fig. 4 A summary of common XRD quantification methods [11].

3 Results and Discussion

3.1 Effect of Powder Sample Preparation

Rock samples of FBST and ILST were selected to investigate impact of sample preparation on XRD analysis.

- FBST was difficult to crush with traditional hand method and was placed under tensile test machines. The planetary ball mill machine, (Fig. 5), has about 36 balls for grinding sample. Pulverized sample was recovered from FBST with some particles remained after 15 minutes of grinding.
- As for the ILST sample, whereas it was difficult to get pulverized sample after 10 minutes of grinding, the grinded powders became sticky and glued to the grinding bowl (Fig. 5).



Fig. 5 Sample grinding with a mill machine; (Top, Bottom Left) ILST and (Top, Bottom Right) FBST.

Surprisingly, XRD results show that grinding FBST sample from 5 to 15 minutes impacts the results, i.e., there is a contamination from grinding balls into the sample as observed from XRD diffractogram, which demonstrates increasing anomaly signals as grinding time increases (Fig. 6). Such contamination may affect the reading with a rare element Qusongite (WC, tungsten carbide).

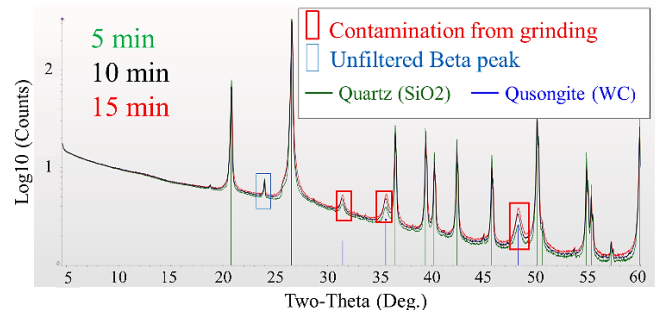


Fig. 6 Effect of rock sample grinding time on XRD diffractogram – FBST (Fontainebleau sandstone).

Manual grinding (pestle and mortar) has been the traditional way of preparing powdered sample. However, for most rock samples it is difficult reaching grain size of 10 μm by such a manual method. The results of FBST samples prepared by manual and machine grinding clearly indicate the machine contamination (red rectangles in Fig. 7).

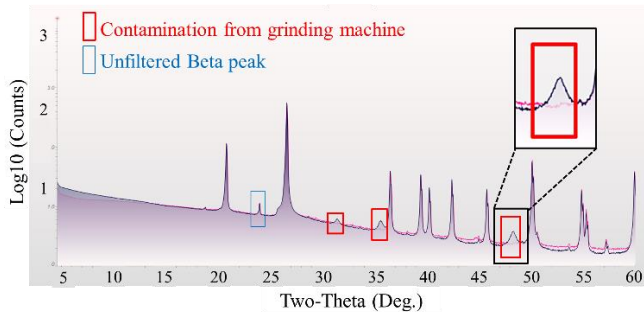


Fig. 7 XRD diffractogram for samples prepared by manual (red) and machine (dark) grinding- FBST samples. Red boxes indicate contamination from grinding machine.

On the other hand, for the ILST sample, no machine grinding contamination was observed (Fig. 8), indicating that XRD sample preparation is rock type driven. Different sample preparation methods may be used for rocks with different lithologies, cementations, and rock mechanical properties.

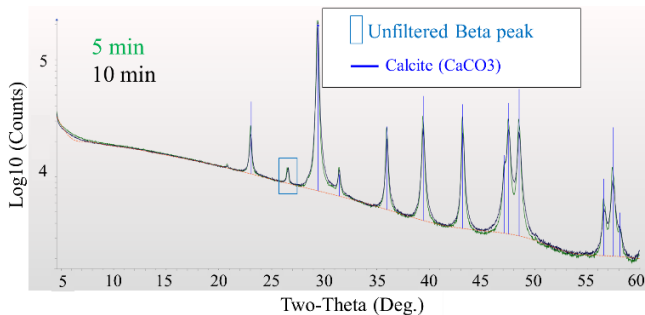


Fig. 8 Effect of grinding time on XRD diffractogram- ILST (Indiana Limestone).

3.2 Effect of Machine and Data Acquisition Parameter

3.2.1 Effect of XRD Machine

Different equipment may be used for XRD tests by different laboratories. To evaluate potential impact of using different machines on XRD data acquisition, the above (Figs. 6-8) diffractograms presented unfiltered K_{β} peak at roughly 2θ =around 25 deg ranging from 23 to 27 deg which may not be reflecting minerals in the sample.

The characteristic X-rays as shown in Fig. 9 as two sharp peaks occurring when vacancies are produced in the $n=1$ or K-shell of the atom.

- The X-rays produced by transitions from level $n=2$ to $n=1$ are called K_{α} X-rays.
- The X-rays produced in the transition from $n=3$ to $n=1$ is called K_{β} x-rays [13], which is considered a spectral contamination in the diffraction patterns.

The unfiltered K_{β} peak is related to XRD instrument malfunction. For example, the Rigaku machine is equipped with a filter to suppress the K_{β} peak, but occasionally, the filtering may not work properly. Consequently, inexperienced XRD data interpreter may mistake this K_{β} peak a mineral phase, thereby introduce false positive mineral in the XRD result.

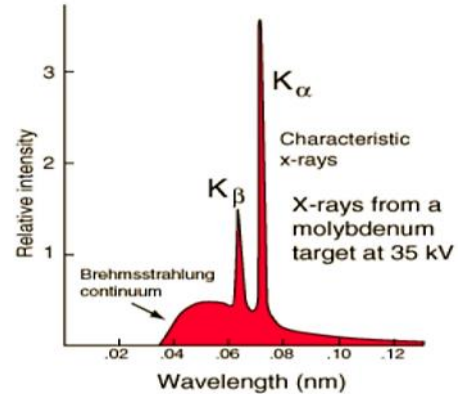


Fig. 9 Schematic emission spectrum of X-rays [13].

The results from two XRD machines were compared in Fig. 10. Diffractogram of CSST shaly sample from Panalytical machine (green) shows better result when compared to Rigaku machine (dark), as the former provides clear peaks and lower counts offset, probably due to the lower step-size (Table 1) associated to the Panalytical machine (0.01 deg) than that of the Rigaku machine (0.02 deg), which minimizes the impact of sample's graininess.

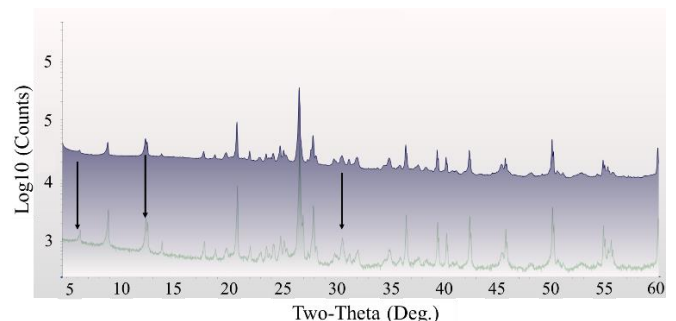


Fig. 10 XRD diffractogram of CSST shaly sample prepared by machine grinding. Data acquired from Rigaku (dark) and Panalytical (green) machine can be different.

3.2.2 Effect of Data Acquisition

Changing data acquisition parameter settings such as scanning speed may also affect the measurement raw data. As shown in Fig. 11, data intensity count drastically increased when scan speed (defined as the time spend at an analysis point) is doubled from 1.2 to 2.4 second. Note that the start angle is the angle at which the machine starts the analysis and stops at the end angle (in this case, 4.6° to 60°). Sample weight is the step size in degree at which the machine takes a measurement.

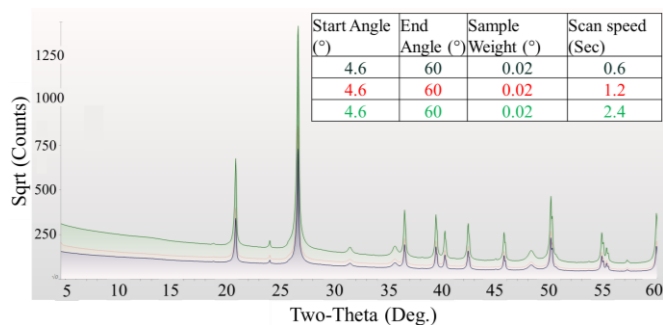


Fig. 11 Examples of XRD diffractogram with varying scanning speed- FBST sample.

3.3 Effect of Sample Lithology

Three Chelsea sandstone CSST samples were prepared to investigate impacts of sample grain size and lithology on the XRD tests. As indicated in Fig 12, the high background in the sideritic sandstone (red diffractogram) affected the measurement (green diffractogram) due to the secondary copper radiation associated with the iron containing materials. The dark diffractogram from the shaly (50% of shaly and sideritic) sandstone showed multiple mineral phases which are repressed in the green diffractogram.

In XRD analysis, the Cu K_α radiation is the most widely used, but samples that are rich in Fe, Cr, and Mn will fluoresce under the incident Cu K_α beam and create polychromatic radiation [14, 15], leading to abnormal shaped and elevated backgrounds as observed in Fig. 12.

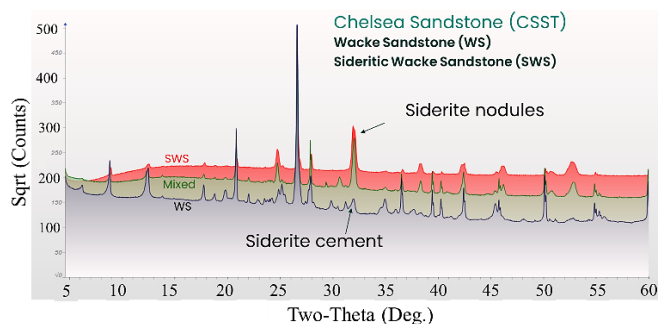


Fig. 12 XRD diffractograms of CSST samples prepared by automated machine grinding, shaly unit (dark), sideritic unit (red) and 50% their mixture (green). Data acquisition with a Rigaku machine.

3.4 Mineral Phase Identification

The general method of identifying mineral phases in XRD test is by using a mineral database such as ICDD PDF4+ and a specialized software with searching and matching capabilities, such as by line match points between measured data and ICDD PDF4+ database. With thousands of minerals in the database, the major challenge in the success of mineral matching is the quality of the measured XRD data. In addition, to use such search/match software efficiently and constrain the matching process, some prior knowledge of basic sample mineralogy is a requirement so that an expert operator can select the range of expected patterns in the database.

Another challenge is mineral phase overlapping; a very common issue especially with clay minerals. Illite and muscovite for example belong to the same mica group, thus are difficult to separate in mineral phase identification. To demonstrate this, a systematic line match approach was used on CSST sample to assess the match of both minerals. As shown in Figs. 13 and 14, it is observed that the illite primary peak 100% (refers to 100% intensity count) matched well with the raw data thus may be considered it is present in the sample. The next secondary peak (at 86%) cannot be identified from the background noise (Fig. 13), indicating absence of illite mineral in the sample. Whereas in the muscovite phase, all peaks matched well with the raw data (Fig. 14).

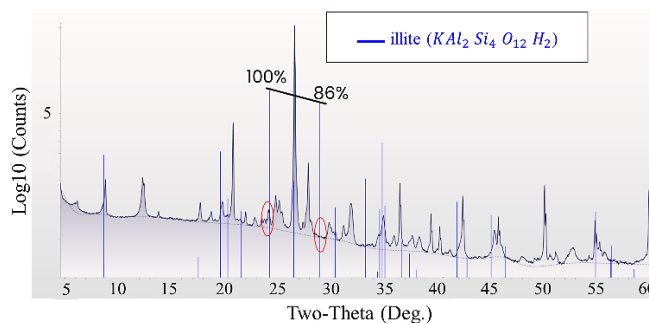


Fig. 13 XRD diffractograms of CSST shaly unit sample with illite phase from database for phase identification. Red circles show key consideration line for data matching.

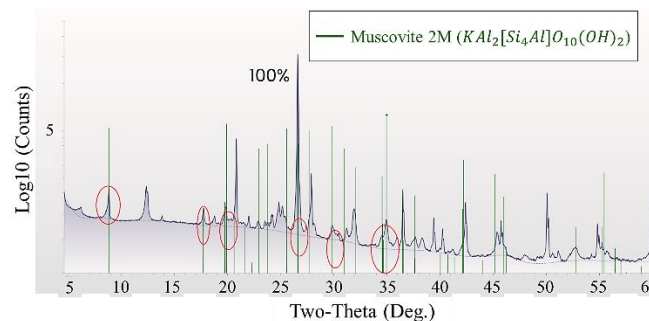


Fig. 14 XRD diffractograms of CSST shaly unit sample with muscovite 2M phase from database for phase identification. Red circles show key consideration line for data matching.

Although mineral phase identification depends on computing power and the quality of the information available in the library, an experienced powder diffraction specialist on the other hand will also be required to better differentiate signals from noises.

As a general guideline, the following steps are recommended for proper mineral phase identification:

1. Sample background information: It is important to understand the source of the sample to minimize error during searching/matching between the sample and those in the database.
2. It is obvious that a robust mineral searching/matching software and a rich database with vast minerals are a

must to process the raw data and matching with minerals in the database.

3. Mineral phase association: to ensure matching is unique, mineral phase association is another important consideration, since many metamorphic, igneous, and sedimentary minerals have similar crystal structure that may confuse the analyst.
4. And lastly, an intuitive peak matching technique to separate overlaps.

3.5 Mineral Phase Quantification

3.5.1 Effect of Simulation Models

To assess effect of simulation model on mineral phase quantification, the sample of Indiana Limestone (ILST) and ICDD PDF4+ are used as an example. One aspect of the assessment is to calculate the goodness of fit (GoF); defined as the average difference between the measured data and the simulated one, and the smaller the GoF value, the better fit.

For ILST, we expect to observe almost 100% calcite mineral. The Variable Spline simulation model fitting indicates 98.3% calcite and a trace of 1.7% quartz with GoF=11.67 (Fig. 15). With the same experimental data, if the Refinable Polynomial (RPoly) simulation model is used, GoF is improved from 11.67 down to 7.12, but with the cost of introducing more weight to quartz 9.2% (or 90.8% calcite); uncommon for Indiana limestone outcrop. With further investigation, it was observed that additional trace signals introduced in the simulated XRD data (Fig. 16), marked in green, affected the calculation of mineral weights. The results of Current

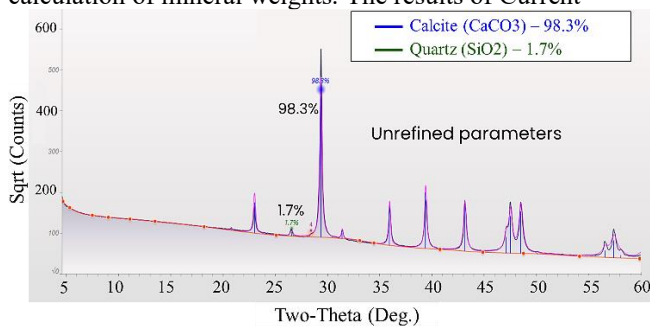


Fig. 15 XRD diffractogram with Variable Spline simulation model for phase quantification, raw data (Black) vs simulated data (Pink)- ILST sample

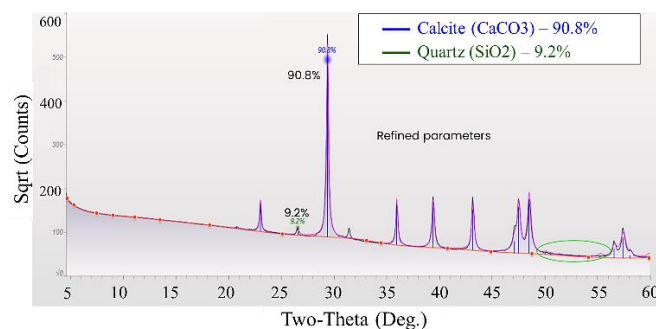


Fig. 16 XRD diffractogram with RPoly simulation model for phase quantification, raw data (Black) vs simulated data (Pink)- ILST sample.

Background (BG) simulation model is consistent with Variable Spline as to be illustrated in the following sections.

To investigate this issue further, measurement of a multiminerall mixed (MIX1) sample is conducted and different simulation models were assessed (Figs. 17 and 18). It is observed both models provided good match except for mineral Albite where RPoly overweighs Variable Spline method by 1.4 wt% (Fig. 19). It is also noticed that the GoF values for both simulations are quite similar; 6.23% for RPLY and 6.08% for Variable Spline, indicating that sample complexity in terms of minerals may sometimes present more consistent results than pure and single mineral samples as in the case of ILST.

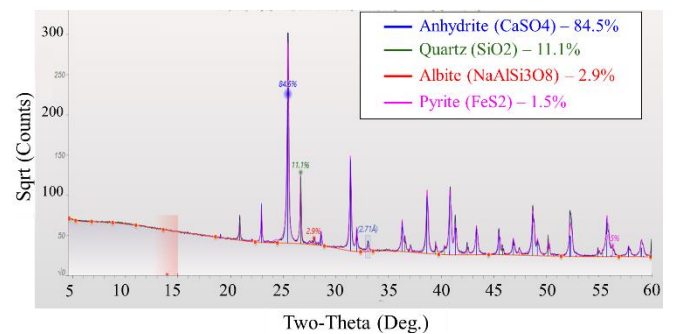


Fig. 17 XRD diffractogram with Variable Spline simulation model for phase quantification, raw data (Black) vs simulated data (Pink)-mixed sample (MIX1).

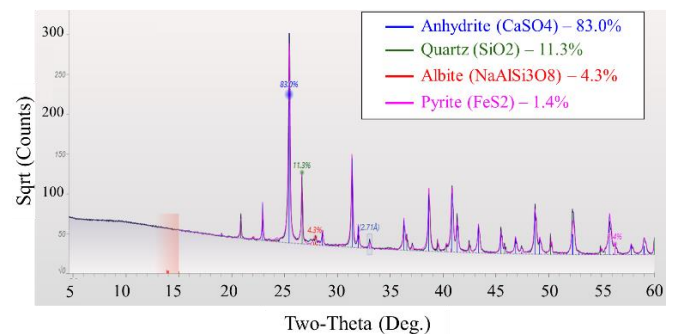


Fig. 18 XRD diffractogram with RPoly simulation model for phase quantification, raw data (Black) vs simulated data (Pink)- mixed sample (MIX1).

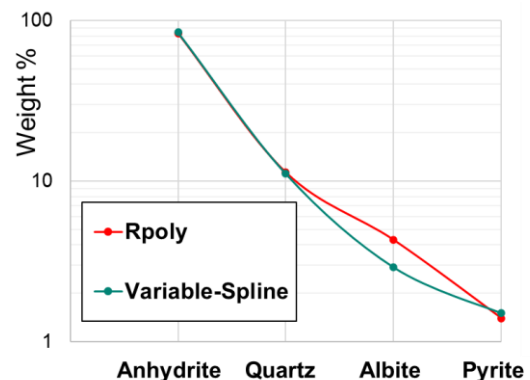


Fig. 19 Minerals analysis produced from two different simulation models applied on the same XRD data (Figs. 17 and 18) of the mixed sample (MIX1).

3.5.2 Effect of Sample Heterogeneity and Minerals

To study the impacts of minerals and sample heterogeneity to mineral quantification, we evaluated the Fe-rich sample CSST. Since the sample is heterogenous in minerals distribution (Fig. 20), three samples were prepared and measured (ref to Fig. 12). Here, we evaluated the effect of simulation models on each sample and utilizing AMCSO library first. Starting with the Wacke sandstone (WS) which is extracted from low Fe side of CSST, where it is expected to see low Sideritic content, and the modeled results agree as expected (Fig 21). However, for clay minerals on same WS sample, quite large discrepancy between the simulation models was observed with variation as large as 10wt% for chlorite. For kaolinite, the Current Background (BG) and Variable-Spline models match each other and deviate from RPoly model by about 5wt% (Figure 21).



Fig. 20 Different views of the CSST sample showing spatial variation in mineralogy with dark brown areas representing Fe-rich content (Siderite).

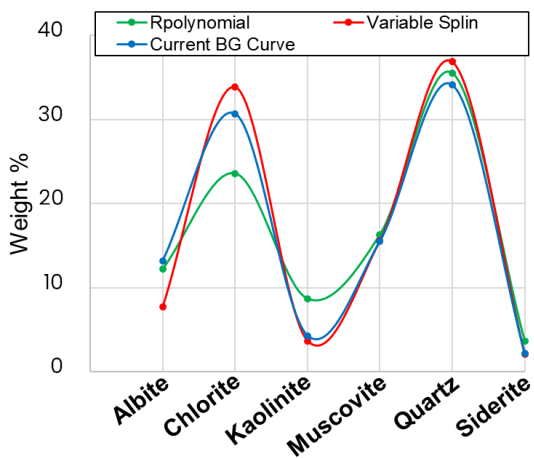


Fig. 21 Minerals analysis as produced from three different simulation models applied on the same Wacke sandstone (WS) XRD data shown in Figure 12.

3.5.3 Effect of Database Library of Minerals

To test the sensitivity of XRD results with respect to database libraries of standard minerals, Fig. 22 shows the results of using three libraries (PDF4+, MDI, and AMCSO) with three simulation models (Rpolynomial, Variable Spin, and Current BG curve). From Fig. 22, it is observed that both PDF4+ and MDI libraries provide consistent results as compared with AMCSO library, though the later performed the best as measured by GoF for quality of matching of measured data with that in the libraries (Table 2), suggesting that one should be careful in using GoF value as a quality control. In addition,

as an example of to quantify the impact of mineral libraries, mineral grain density is calculated (Table 2), and it shows that AMCSO library provides lower mineral grain density compared to PDF4+ and MDI libraries.

Qualitatively, it is obvious that the sample standards of chlorite and muscovite in AMCSO are drastically different from that in the other two libraries, and those may have affected the value of derived quartz content, as summarized quantitatively in Table 3, since both phase identification and quantification are affecting each other.

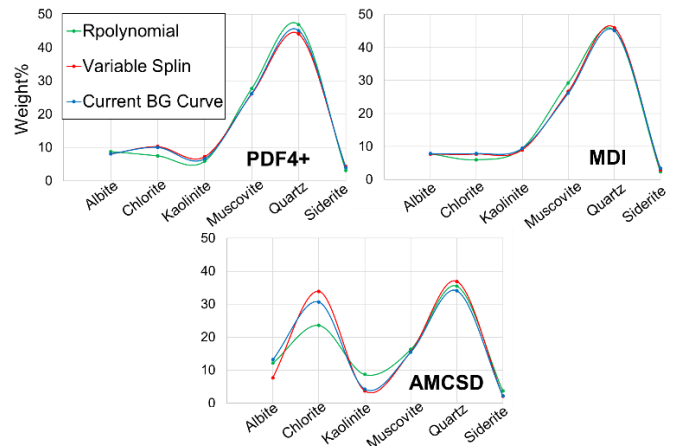


Fig. 22 Minerals analysis from three different simulation models with three different libraries for the Wacke sandstone (WS) sample (Fig. 12).

Table 2 Summary of effects of simulation models and minerals libraries on XRD data processing performance (GoF) and XRD data as exemplified by grain density (ρ_g in g/cc)- WS sample

	RPoly		Variable Spline		Current BG Curve	
	GoF	ρ_g	GoF	ρ_g	GoF	ρ_g
MDI	7.94	2.7154	8.36	2.7176	7.81	2.7207
PDF4+	6.29	2.7209	6.65	2.7305	6.47	2.7282
AMCSO	5.67	2.7088	5.64	2.7029	5.78	2.6981

Table 3 Effect of libraries on mineral averaged from three models (RPoly, Variable Spline, and Current BG curve)

	PDF4+	MDI	AMCSO
Albite (wt%)	9	8	11
Chlorite (wt%)	9	8	27
Kaolinite (wt%)	7	9	7
Muscovite (wt%)	28	28	17
Quartz (wt%)	46	47	35
Siderite (wt%)	3	3	3

As another example, a Fe-rich sample labeled as sideritic wacke sandstone (SWS) is taken to study effect of mineral library and simulation model on extracted XRD data (Fig. 23). Visually, Rpolynomial model cannot handle the Fe-rich sample; struggling with all three mineral libraries. As to the effect of the mineral libraries, AMCSO again shows abnormal behavior for Chlorite and Muscovite.

The simulation modeling performance indicator GoF and modeled mineral grain density are summarized in Table 4.

Without considering the Rpolynomial results, modeled XRD mineralogy by using the two models of Variable Spline and Current BG curve are summarized in Table 5 to illustrate the impact of mineral libraries. Like for the WS sample, using the AMCSD library over-estimate Chlorite and under-estimate Muscovite compared to PDF4+ and MDI libraries.

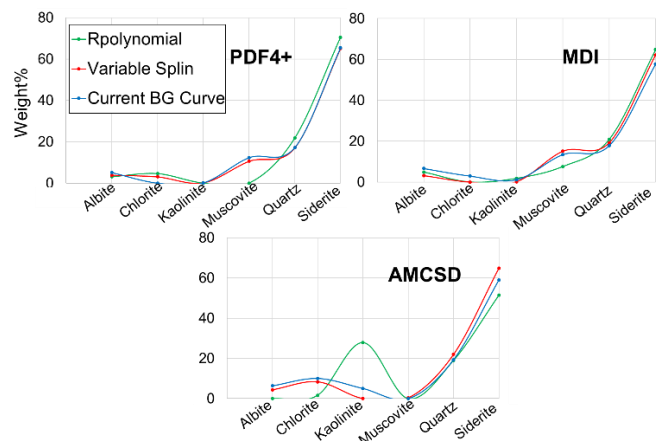


Fig. 23 Minerals Analysis as produced from three different simulation models and three different libraries applied on the same Sideritic Wacke sandstone (SWS) XRD data shown in Fig. 12.

Table 4 Summary of effects of simulation models and minerals libraries on XRD data processing performance (GoF) and XRD data as exemplified by grain density (ρ_g in g/cc)- SWS sample

	RPoly		Variable Spline		Current BG Curve	
	GoF	ρ_g	GoF	ρ_g	GoF	ρ_g
MDI	4.89	3.3616	3.03	3.3461	3.89	3.2814
PDF4+	4.94	3.4299	2.81	3.3797	2.7	3.3866
AMCSD	3.65	3.1507	2.23	3.3533	1.88	3.2638

Table 5 Effect of libraries on mineral averaged from the two models (Variable Spline and Current BG curve)

	PDF4+	MDI	AMCSD
Albite (wt%)	5	5	6
Chlorite (wt%)	2	2	9
Kaolinite (wt%)	0	1	4
Muscovite (wt%)	11	15	0
Quartz (wt%)	17	18	20
Siderite (wt%)	65	60	62

4. Summary and Recommendations

Based on this evaluation study of XRD mineralogy measurements, the following are summarized;

- Depending on sample mineralogy and the grinding material, sample grinding machine may introduce contamination, thus noise to the raw data.
- Equipment malfunction may also generate noise peaks, which may cause data misinterpretations.
- Thus, careful distinction between noises and mineral phase peaks and phase associations are crucially important, and occupationally may be challenging.

It is therefore recommended

For sample preparation

- Careful quality control of sample preparation for consistence, repeatability, and data quality.

For mineral phase identification

- Acquire information about the geological background of the sample to be tested.
- Pay special attention to the knowledge of Fe minerals in case of using Cu radiation source.
- Ensure the library of minerals standards is robust.
- Careful select the mineral searching and matching simulation model for mineral identification.

Mineral phase quantification

- Mineral libraries need to be tested for sensitivity, especially for samples contains clays.
- Sensitivity of mineral search and matching simulation models need to be tested extensively to ensure its capability in quantifying common and rare minerals with accuracy, precision, and consistency.

Nomenclature

Abbreviations

AMCSD= American Mineralogist Crystal Structure Database
 FBST= Fontainebleau Sandstone
 CSST= Chelsea Sandstone
 ICDD= The International Centre for Diffraction Data
 ILST= Indiana Limestone
 MDI= Materials Data, Inc
 PDF4+= Powder Diffraction File 4+
 RPoly= Refined Polynomial
 SWS= Sideritic Wacke Sandstone
 WS= Wacke Sandstone
 XRD= X-Ray Diffraction
 GoF= Goodness of Fit

Symbols

λ = incident X-ray wavelength.
 n = an integer (i.e. 1, 2, 3, etc.).
 d = distance between lattice planes.
 θ = angle between the incident X-ray and the lattice plane.
 I_{hkl} = the integrated intensity of a reflection with Miller indices (hkl).
 k = a scaling constant related to the intensity of X-ray beam.
 L_p = the Lorentz & X-ray polarization factor which is dependent on the Diffraction Geometry.
 T = the overall temperature factor of the structure.
 A = the absorption correction for flat and thin specimen.
 G = the preferred orientation correction.
 m = the reflection multiplicity.
 F_{hkl} = the structure factor derived from the packing (i.e. Fourier transform) of all atoms in the unit cell.
 K_α = X-rays produced by transitions from the $n=2$ to $n=1$ levels.
 K_β = The X-rays produced in the transition from $n=3$ to $n=1$ levels.

Acknowledgement

This work was mainly conducted by Dr. Maaruf Hussain, who tragically lost his life during the late stage of the study. The authors are grateful to KFUPM for the use of some laboratory facilities to conduct part of the study. Special thanks to Rajaa, Gonzalo, Syed Ali for assistance with samples preparation. Thanks also go to Ahmed Abouzaid, Nora Alacron and Jerome Zhang for technical discussions, and to Ahmed AlZoukani for his critical review.

References

1. S. Ma, A. Al-Muthana, & R. Dennis. Use of Core Data in Log Lithology Calibration: Arab-D Reservoir, paper SPE 77778, Oct 2002.
2. T. Liang, Z.W. Zhan, Y.R. Zou, X.H. Lin, P. Peng. Interaction between Organic Solvents and Three Types of Kerogen Investigated via X-ray Diffraction. *Energy & Fuels*, **36** (3), 1350-1357, 2022.
3. W. Kaczmarczyk, M. Słota-Valim, Multidisciplinary Characterization of Unconventional Reservoirs Based on Correlation of Well and Seismic Data. *Energies*, **13**, 4413, 2020.
4. G.A Barberes, R. Pena dos Reis, N.L. Pimentel, A.L.D. Spigolon, P.E. Fonseca, P. Karcz, M.C. Azevedo, M.T. Barata, Geochemical Considerations from the Carboniferous Unconventional Petroleum System of SW Iberia. *Minerals*, **11**, 811, 2021.
5. A. Rahfeld, R. Kleeberg, R. Möckel, J. Gutzmer, Quantitative mineralogical analysis of European Kupferschiefer ore. *Miner. Eng.*, **115**, 21—32, 2000.
6. O'Brien, N.R. Fabric of Kaolinite and Illite Floccules. *Clays Clay Miner*, **19**, 353–359, 1971.
7. Y. Uvarova, J. Cleverley, M. Verrall, A. Baensch, Coupled XRF & XRD analyses for rapid and low-cost characterization of geological materials in the mineral exploration & mining industry, *Explore*, **162**, 4-14, 2014.
8. D. A. Burkett, I. Graham, C. R. Ward, The application of portable X-ray diffraction to quantitative mineralogical analysis of hydrothermal system, *Can. Mineral.*, **53**, 429—454, 2015.
9. Eby, G.N., Principles of Environmental Geochemistry. *Brooks/Cole-Thomson Learning*, 212—214, 2004.
10. L. D. Barbara, M.C. Christine, X-ray Powder Diffraction https://serc.carleton.edu/msu_nanotech/methods/XRD.html, 2022.
11. I.C. Madsen, N.V. Scarlett, A. Kern, Description and survey of methodologies for the determination of amorphous content via X-ray powder diffraction. *Z. Krist.*, **226**, 944–955, 2011.
12. N. Scarlett, I. Madsen, Quantification of phases with partial or no known crystal structures. *Powder Diffraction*, **21**(4), 278–284, 2006.
13. Debjani B. presentation: (Source from <https://www.iitk.ac.in/che/pdf/resources/XRD-reading-material.pdf>)
14. C.Y. Lin, A.V. Turchyn, A. Krylov, G. Antler, The microbially driven formation of siderite in salt marsh sediments. *Geobiology*, **18**(2), 207–224, 2020.
15. F.R.D. de Andrade, L. de Andrade Gobbo, L.F.A. Sousa, Iron ore classification by XRD-Rietveld and cluster analysis. *Geo. USP. Série Cient.*, **16**(2), 19–24, 2016.
16. L.A.M. Montoya, Automatic reduction of large x-ray fluorescence data-sets applied to XAS and mapping experiments. Doctoral degree thesis, Universitat Paderborn, 2016.